HHS Public Access

Author manuscript

Clin Cancer Res. Author manuscript; available in PMC 2020 July 15.

Published in final edited form as:

Clin Cancer Res. 2019 July 15; 25(14): 4552–4566. doi:10.1158/1078-0432.CCR-17-0375.

High-throughput Chemical Screening Identifies Focal Adhesion Kinase and Aurora Kinase B Inhibition as a Synergistic Treatment Combination in Ewing Sarcoma

Sarah Wang[1], **Elizabeth E. Hwang**[1], **Rajarshi Guha**[2], **Allison F. O'Neill**[1], **Nicole Melong**[3], **Chansey J. Veinotte**[3,4], **Amy Conway Saur**[1], **Kellsey Wuerthele**[1], **Min Shen**[2], **Crystal McKnight**[2], **Gabriela Alexe**[1,5], **Madeleine E. Lemieux**[6], **Amy Wang**[2], **Emma Hughes**[2], **Xin Xu**[2], **Matthew B. Boxer**[2], **Matthew D. Hall**[2], **Andrew Kung**[7], **Jason N. Berman**[3,4], **Mindy I. Davis**[2,*], **Kimberly Stegmaier**[1,*], and **Brian D. Crompton**[1,*]

[1]Dana-Farber/Children's Hospital Cancer Center, Boston, MA, USA

[2]National Center for Advancing Translational Sciences, Bethesda, MD, USA

[3]IWK Health Centre, Halifax, NS, Canada

[4]Dalhousie University, Halifax, NS, Canada.

[5]Boston University Bioinformatics Graduate Program, Boston, MA, USA

[6]Bioinfo, Plantagenet, ON, Canada.

[7]Memorial Sloan Kettering Cancer Center, New York, NY, USA

Abstract

Purpose: Ewing sarcoma is an aggressive solid tumor malignancy of childhood. Although current treatment regimens cure approximately 70% of patients with localized disease, they are ineffective for most patients with metastases or relapse. New treatment combinations are necessary for these patients.

Experimental Design: Ewing sarcoma cells are dependent on focal adhesion kinase (FAK) for growth. To identify candidate treatment combinations for Ewing sarcoma, we performed a small-molecule library screen to identify compounds synergistic with FAK inhibitors in impairing Ewing cell growth. The activity of a top-scoring class of compounds was then validated across multiple Ewing cell lines *in vitro* and in multiple xenograft models of Ewing sarcoma.

Results: Numerous Aurora kinase inhibitors scored as synergistic with FAK inhibition in this screen. We found that Aurora kinase B inhibitors were synergistic across a larger range of

[*]**Corresponding authors:**Brian D. Crompton, MD, Dana-Farber Cancer Institute, 450 Brookline Avenue, Boston, Ma 02215, Phone: (617) 632-4468, Fax: (617) 632-4850, briand_crompton@dfci.harvard.edu, Kimberly Stegmaier, MD, Dana-Farber Cancer Institute, 450 Brookline Avenue, Boston, Ma 02215, Phone: (617) 632-4438, Fax: (617) 632-4850, kimberly_stegmaier@dfci.harvard.edu, Mindy I. Davis, PhD, National Center for Advancing Translational Sciences, 9800 Medical Center Drive, Rockville, MD, 20850, Phone: (301) 480-9928, Fax: (301) 217-5736, mindy.davis@nih.gov.

Conflict of Interest Statement: K.S. participates in the DFCI/Novartis Drug Discovery Program, which includes grant support for an unrelated project, and consults for Rigel Pharmaceuticals on a topic unrelated to this manuscript. B.C. receives funding from Gradalis, Inc. for a project unrelated to this manuscript and his spouse is employed by Acceleron Pharma for which there is no known conflict of interest.

concentrations than Aurora kinase A inhibitors when combined with FAK inhibitors in multiple Ewing cell lines. The combination of AZD-1152, an Aurora kinase B-selective inhibitor, and PF-562271 or VS-4718, FAK-selective inhibitors, induced apoptosis in Ewing sarcoma cells at concentrations that had minimal effects on survival when cells were treated with either drug alone. We also found that the combination significantly impaired tumor progression in multiple xenograft models of Ewing sarcoma.

Conclusions: FAK and Aurora kinase B inhibitors synergistically impair Ewing sarcoma cell viability and significantly inhibit tumor progression. This study provides preclinical support for the consideration of a clinical trial testing the safety and efficacy of this combination for patients with Ewing sarcoma.

Keywords

Ewing sarcoma; focal adhesion kinase; Aurora kinase; combination therapy; zebrafish; xenograft models; cellular responses to anticancer drugs; kinase inhibitors

Introduction

Ewing sarcoma is the second most common pediatric bone malignancy of childhood. Therapy for newly diagnosed patients consists of systemic treatment with repeated cycles of chemotherapy combined with either surgical resection, radiation therapy, or both. Recent efforts to improve outcomes for patients who present with non-metastatic disease by intensifying therapy have resulted in only a modest increase in 5-year event-free survival (EFS) suggesting that additional attempts to intensify therapy may have only limited efficacy (1). For patients with metastatic disease at diagnosis, chemotherapy intensification has done little to improve outcomes with an expected 5-year EFS of approximately 20% (2). Thus, new classes of treatment are needed for patients with Ewing sarcoma.

The hallmark molecular aberration identified in Ewing sarcoma tumors is the presence of genomic rearrangements of *TET*-family genes with *ETS*-family transcription factor genes. The resulting fusion protein, most commonly EWS/FLI, is believed to be the oncogenic driving event in this disease (3). However, pharmacologic modulation of transcription factors has been notoriously challenging, and direct inhibitors of EWS/FLI have yet to be successfully applied in the clinic. While there was great hope that genomic profiling of Ewing sarcoma tumors would reveal recurrent somatic dependencies more readily tractable with targeted inhibitors, recent studies demonstrated that these tumors are among the most genomically stable human cancers (4). These studies also demonstrated a stark paucity of recurrently mutated genes currently considered targetable by available anti-cancer therapies (5,6).

To identify new therapeutic approaches for Ewing sarcoma, we previously utilized a proteomic approach to identify molecular dependencies that may be more amenable to direct inhibition. We determined that Ewing sarcoma cells are dependent on focal adhesion kinase (FAK) *in vitro* and in mouse xenograft models of this disease (7). FAK is a non-receptor tyrosine kinase that promotes cellular growth, survival and migration. FAK expression and activity in cancer have been associated with poor outcome and inhibitors of FAK are under

active clinical investigation (8,9). Recognizing that single-agent targeted therapy is rarely curative in cancer, we performed a small-molecule library screen of Ewing sarcoma cell lines to identify additional targetable dependencies that, when inhibited, synergistically impair cell viability in combination with FAK inhibition. We demonstrate that Aurora Kinase B inhibitors are a class of compounds that act synergistically with FAK inhibitors to impair cell viability in Ewing sarcoma cell lines and suppress tumor progression and improve survival in xenograft models of Ewing sarcoma.

Materials and Methods

Small-molecule library drug combination screening

A high-throughput screen was conducted in 1536-well white flat bottom plates (Corning) on a Kalypsys robotic system. Using a MultiDrop Combi (Thermofisher Scientific), 2 μL of media were added to the plates. Compounds were dissolved in DMSO and then added to plates using the EDC ATS100 acoustic dispenser (EDC) creating 6 by 6 matrix blocks using a method described previously (10). Briefly, a 6-concentration-point, three-fold dilution of PF-562271, a selective FAK inhibitor (SynKinase), was transferred to the screen plates by transferring a total volume of 10 nL per well (11). The MIPE 4.0 library (Supplemental Table S1) was also transferred by acoustic dispensing into the same plates with each compound plated in six-point dilution series at five-fold serial dilutions. A673 cells were seeded into plates at a final density of 500 cells in 5 μL of media per well (MultiDrop Combi). After 48 hours of compound incubation, 3 μL of Cell-TiterGlo reagent (Promega) was added to each well. Following a 10 minute incubation, luminescence was read using the Viewlux microplate reader (PerkinElmer). Primary combination screening data is publicly available at https://tripod.nih.gov/matrix-client/?p=442.

Select combinations of interest from the primary screen were retested against a panel of Ewing sarcoma cell lines. Cells were seeded in 384-well white flat bottom plates (Corning) at a final density of 1000 cells in 50 μL of media per well using a robotic dispenser (BioTek). Immediately after plating, media with PF-562271 (Selleck) at a 7-point, two-fold dilution was added robotically by a Bravo Liquid Handler (Agilent) to the plate in combination with media containing either AZD-1152 (Sigma Aldrich) or MLN-8237 (Selleck) at an 11-point, two-fold dilution (12,13). Cells were treated with four replicates of each concentration of each combination. After 48-hours, 10 μL of Cell-TiterGlo reagent (Promega) were added to each well. Luminescence was read using the FLUOstar Omega microplate reader (BMG Labtech). Dose-response curves for each individual compound were generated from wells in microtiter plates treated with only one compound. Cell culture conditions, cell line verification and analysis of drug synergy are detailed in the Supplemental Material.

Gene expression analysis

Gene expression data for *AURKA* and *AURKB* were extracted from previously published transcriptome sequencing of 23 primary Ewing sarcoma tumors and 9 Ewing sarcoma cell lines (5). *AURKA* and *AURKB* gene expression data were also extracted from The Cancer Genome Atlas (TCGA; http://cancergenome.nih.gov) (14). *AURKA* and *AURKB* expression

were also downloaded from the Cancer Cell Line Encyclopedia (CCLE; http://portals.broadinstitute.org/ccle) (15). One-way ANOVA with ranks test was used to compare expression of genes in tumor subtypes. A two-tailed unpaired t-test was used to compare gene expression of genes in Ewing sarcoma cell lines to all others. Analyses were performed in Prism 6 (GraphPad).

Genomics of Drug Sensitivity in Cancer data analysis

Publicly available cell line treatment data and analyses were accessed at the Genomics of Drug Sensitivity in Cancer Project website (http://www.cancerrxgene.org) on July 2016, Release 6 (16). Data and analyses were downloaded in three ways 1) EWS/FLI as a predictor of sensitivity to all drugs, 2) cancer features predicting sensitivity to GSK-1070916 and 3) IC_{50} of all cell lines treated with GSK-1070916 (17). The half-maximal inhibitory concentration (IC_{50}) of the Ewing sarcoma cell lines treated with GSK-1070916 was compared to all other cell lines by a two-tailed Mann-Whitney test. Downloaded data were plotted and analyzed in Prism 6 (GraphPad).

Ewing sarcoma cell line dependency analysis

To determine the dependency of Ewing sarcoma cell lines on AURKB, data from the Broad Institute's Achilles Project v2.4.3 were analyzed (www.broadinstitute.org/achilles) (18). The Achilles Project utilized an RNAi library of 56,903 barcoded shRNAs targeting 14,222 genes. A collection of 216 cancer cell lines, including 5 Ewing sarcoma lines, were transduced with this library and after 16 cell doublings, cells were assessed for relative enrichment or depletion of shRNAs. The dataset contained three hairpins targeting AURKB (Supplemental Table S2). Ewing sarcoma dependencies were scored with the RIGER method using Gene-E v3.0.204 (www.broadinstitute.org/cancer/software/GENE-E) (19). Individual hairpins were ranked by their average dependency across the Ewing sarcoma cell lines based on a z-score. Gene-level depletion scores were computed from the weighted sum of the z-scores for the first (weight of 0.25) and the second (weight of 0.75) ranked hairpins for that gene and the significance was assessed by permutated P-value.

In vivo Ewing sarcoma dependency screen

A list of 449 potential putative chromatin regulatory genes was compiled using 1) an NCBI Gene Ontology Annotation Database search with terms including: epigenetic regulation of gene expression, chromatin modification, histone binding, histone kinase, and histone modification and 2) a search of the UniProt database for genes with functional domains associated with epigenetic regulation. A collection of shRNA pLKO.1 constructs was assembled from the Broad Institute's Genetic Perturbation Platform (http://portals.broadinstitute.org/gpp/public/) such that 7–8 shRNAs were included per gene plus 12 control shRNAs, totaling approximately 3000 shRNAs. The collection included 7 hairpins targeting AURKB (Supplemental Table S3).

For lentivirus production, HEK-293T cells were transfected using the X-tremeGene HP DNA Transfection Reagent protocol (Roche). Lentiviral vector and packaging plasmids (pCMV8.9 and pCMV-VSVG) were transfected along with shRNA expressing plasmids. Cell lines were transduced with the pooled lentiviral shRNA library and selected with

puromycin 12 hours post-transduction. After cells were cultured for 7–10 days post-selection, 10 million cells were collected as an “input” sample. Simultaneously, 1 million cells suspended in 30% matrigel were injected subcutaneously in 5 NOD SCID gamma (NSG) mice. Once tumors reached 500 mm^3, mice were sacrificed and DNA was extracted from each tumor and the input samples using a DNeasy Blood and Tissue Kit (Qiagen). DNA was amplified using nested multiplex PCR with barcoded primers specific to the target region of each shRNA. PCR products were purified and sequenced. Hairpin abundance was estimated by determining the counts-per-million (CPM) of each hairpin barcode identified. We used Wilcoxon rank order tests corrected for multiple hypothesis testing by Benjamini-Hochberg method to identify significant changes in CPM relative to input for individual hairpins or at the gene level by combining all hairpin counts for a given gene.

Downregulation of Aurora kinase, FAK, and EWS/FLI expression

Aurora kinase, FAK, and EWS/FLI expression were downregulated by transducing cells with either CRISPR Cas9 gene editing plasmids or inducible shRNA plasmids packaged in lentivirus as described above. For CRISPR studies, target guides were designed using the Broad Institute Genetic Perturbation Platform’s sgRNA design tool (www.broadinstitute.org/rnai/public/analysis-tools/sgrna-design). Selected guides (Supplemental Table S4) were cloned into the lentiCRISPR V2 plasmid (Addgene) as previously described (20). Inducible shRNA plasmids were obtained from Dharmacon (GE; Supplemental Table S5). For transduction, Ewing cells were incubated for two hours with 2 mL of virus and 8 μg/mL polybrene. Cells were selected with puromycin two days after transduction. Cells transduced with inducible shRNA plasmids were transferred two days later to medium containing puromycin and 1 μg/mL of doxycycline. Experiments were initiated within three to five days of puromycin selection and, for cells with inducible plasmids, two days after the addition of doxycycline. Downregulation of target gene expression was confirmed by western immunoblotting as described in the Supplemental Materials.

Cell viability, apoptosis, cell cycle analysis, and phospho-S6 analysis

To determine the effects of perturbations on Ewing sarcoma cell viability, cells were plated in 384-well plates at a concentration of 1000 cells per well in 50 μL of medium. Cell viability was measured by adding 10 μL of Cell-Titer Glo ATP-based assay (Promega). Luminescence was read using the FLUOstar Omega microplate reader (BMG LabTech). VS-4718, GSK-1070916, and NVP-AEW541 were obtained from Selleck for *in vitro* treatment of cells. Cells undergoing apoptosis were stained with Annexin V using the Apoptosis Detection Kit-APC (eBioscience) and cellular DNA content was measured by propidium iodide staining (Invitrogen). For intracellular phospho-protein staining, cells were fixed and permeabilized using the BD Cytofix/Cytoperm Kit (BD Biosciences) and stained with phycoerythrin (PE) anti-phospho-S6 (S240, BD Biosciences) and analyzed by flow cytometry. A minimum of 10,000 stained cells were analyzed in all flow cytometry experiments. All experiments testing viability, apoptosis, cell cycle, and measurements of phosphorylation of S6 were performed with two or more experimental replicates and each experiment repeated a minimum of two times. Experiments shown are representative of experimental and biologic replicates.

Reverse Phase Protein Array (RPPA) analysis

A673 and TC32 cell lines were treated for 36 hours with FAK inhibitors (PF-562271 and VS-4718 at 2.5 μM) and Aurora kinas B inhibitors (AZD-1152 and GSK 1070916 at 20 nM). Cell pellets were harvested, lysed and quantified, and applied to the chip-based RPPA array and the RPPA assay was performed and analyzed by the M.D. Anderson Cancer Center core facility as previously described (21). Heat maps were generated with Morpheus software (https://software.broadinstitute.org/morpheus/) with normalized protein or phospho-protein levels.

In vivo treatment combination studies

Methods for zebrafish studies and mouse pharmacokinetic and tolerability studies are described in the supplemental material. For all mouse xenograft studies, AZD-1152, PF-562271, and VS-4718 were purchased from MedChem Express. For all studies, AZD-1152 was dissolved in 0.3 M Tris base pH 9.0 and dosed at 25 mg/kg daily by intraperitoneal injection. PF-562271 was dissolved in 0.5% HPMC, 20% Tween80 and administered by oral gavage twice daily at a dose of 100 mg/kg. VS-4718 was dissolved in 0.5% carboxymethyl cellulose and 0.1% Tween 80 in sterile water and administered by oral gavage twice daily at a dose of 50 mg/kg. Mouse xenograft tumor progression and survival studies were approved by the DFCI Animal Care and Use Committee. For cell line xenograft studies, three million A673 cells were collected and injected subcutaneously into the right flank of 7–8 week-old female NCr nude mice (Charles River Laboratories). For patient-derived xenograft (PDX) studies, fragments of tumor were implanted subcutaneously into the right flank of 7 week-old female NCr nude mice (Charles River Laboratories). Tumor volume was monitored using calipers (volume = 0.5 × length × $width^2$). For each study, mice were divided into 4 groups: vehicle control, AZD-1152 alone, FAK inhibitor alone (PF-562271 in the A673 xenograft study and VS-4718 in the PDX study), and AZD-1152 in combination with a FAK inhibitor. In both studies, treatment began when tumors reached at least 100 mm^3, with AZD-1152 on days 1–4 and 8–11 and FAK inhibitor on days 1–14. Tumor volumes were measured twice a week and animals were sacrificed when tumors reached the institutional limit of 2,000 mm^3.

A table summarizing the reagents and chemicals used in this study is available in the Supplemental Material.

Results

High-throughput screen identifies synergistic drug combinations with FAK inhibitors in Ewing sarcoma

To identify new candidate combination treatment approaches with FAK inhibitors in Ewing sarcoma, we performed a high-throughput screen of 1912 compounds in combination with the FAK inhibitor, PF-562271. We screened the Mechanism Interrogation PlatE (MIPE) compound library 4.0, which includes compounds selected for anti-cancer activity, established mechanistic annotation and clinical relevance (Supplemental Table S1). A673 Ewing sarcoma cells were treated with PF-562271 at six concentrations in combination with each compound from the MIPE 4.0 library at six concentrations, resulting in a treatment

matrix of all possible combinations for each compound pair (Figure 1A). Cells were treated for 48 hours and then cell viability was measured. Each treatment matrix was scored by 4 metrics for evidence of synergistic inhibition of cell viability (Supplemental Table S6). We found that seven Aurora kinase inhibitors ranked in the top 5% of compounds when treatment matrices were analyzed for synergy by the sum of excess over highest single agent (HSA) (Figure 1B). We also noted that the top ten scoring Aurora kinase inhibitors in the screen are classified as either pan-Aurora kinase or Aurora kinase B-selective inhibitors (Figure 1B and Supplemental Table S6). Tozasertib, a pan-Aurora inhibitor, is an illustrative example of the synergistic anti-Ewing activity observed in the screen by combining Aurora kinase inhibition with FAK inhibition (Figure 1C). Indeed, we found that multiple dose combinations of tozasertib and PF-562271 in this screen induced synergistic inhibition of A673 cell viability as determined by Combination Index (Figure 1D).

Aurora kinases A and B are expressed in Ewing sarcoma

We next evaluated the expression pattern of Aurora kinases in Ewing sarcoma cell lines and primary tumors. Previous studies have demonstrated that Aurora kinases are highly expressed in many cancer types (22), with Aurora kinase A and B expressed in Ewing sarcoma cell lines (23,24). We examined RNA-Seq data from a recently published collection of 23 primary Ewing sarcoma tumors and 9 Ewing sarcoma cell lines and found that Aurora kinases A and B were highly expressed but Aurora kinase C was not (Figure 1E) (5). We found that Aurora kinase A and B expression were similar to expression levels observed in eight other cancer subtypes available through the TCGA (Supplemental Figure S1A–B) (14). We also found that Aurora kinase B is expressed in a collection of 9 Ewing sarcoma cell lines (Supplemental Figure S1C) and expression was in the upper third of all cancer cell lines in the CCLE, while Aurora kinase A expression was significantly lower than the average expression of cancer cell lines (Supplemental Figure S1D–E) (15).

Anti-Ewing effect of FAK inhibition combined with Aurora kinase A- and B-specific small-molecule inhibitors

Having confirmed that both Aurora kinase A and B are expressed in Ewing sarcoma, we next determined whether inhibition of Aurora kinase A, B, or both were synergistic with FAK inhibitors in Ewing sarcoma. First, we confirmed that Ewing sarcoma cells are sensitive to both Aurora kinase A- and B-specific inhibitors alone. For these experiments, we utilized MLN-8237, an Aurora kinase A-specific inhibitor, and AZD-1152, an Aurora kinase B-specific inhibitor. We chose these compounds for our confirmation experiments because they were the top ranking inhibitors in our initial screen with specificity for each Aurora kinase (Supplemental Tables S1 **and** S6), both have been tolerated in clinical trials and both continue to be actively developed for clinical use (25–31). We treated nine Ewing sarcoma cell lines with MLN-8237 and AZD-1152 across a broad range of concentrations for two days. We found that both inhibitors impaired cell viability at nanomolar concentrations (Figure 1F–G). Slower-growing Ewing sarcoma cell lines did not achieve 90% inhibition of viability after two days of treatment (Figure 1F–G and Supplemental Figure S2A), an anticipated finding because Aurora kinase inhibitors impair cell division. When the slower growing TC32 cell line is treated for 5 days with AZD-1152, 90%

inhibition is achieved at a similar concentration as in the faster growing cells at the two-day time point (Supplemental Figures S2B).

Next, we confirmed that Aurora kinase inhibitors are synergistic with FAK inhibitors in a collection of nine Ewing sarcoma cell lines. Cells were treated with the drug combinations AZD-1152 and PF-562271, AZD-1152 and VS-4718, or MLN-8237 and PF-562271 across a range of concentrations that specifically inhibited the target of each drug (Supplemental Figure S2C–F). Each combination of specific concentrations was tested in quadruplicate. Cells were incubated with each drug for two days and viability was measured. To identify individual dose combinations that were synergistic, we calculated the Combination Index and excess over Bliss Independence based on the average inhibition of viability of the four replicates. In all Ewing sarcoma cell lines treated with AZD-1152 in combination with PF-562271 or VS-4718, we found that a larger range of drug concentrations had a combination index < 0.7 compared to cells treated with MLN-8237 in combination with PF-562271 (Figure 2A–C, Supplemental Figures S3–S4).

Ewing sarcoma cell lines are dependent on Aurora kinase B

One would expect that the most successful drug combinations in the clinic involve drugs that are also active as single agents against that disease. Our own prior work focused on validation of FAK as a therapeutic target in Ewing sarcoma (7). Published studies have supported a dependency of Ewing sarcoma cells on Aurora kinase B activity for viability *in vitro* (24). However, in light of Aurora kinase B emerging as a top target for synergistic inhibition with FAK inhibitors in Ewing sarcoma, we sought to more thoroughly validate this target *in vitro* and *in vivo*. We first searched the Genomics of Drug Sensitivity in Cancer Project database for compounds for which sensitivity was predicted by the expression of EWS/FLI, the genomic feature defining Ewing sarcoma cell lines in this dataset. Indeed, EWS/FLI was the top scoring feature predicting response to GSK1070916, an Aurora kinase B-selective inhibitor, in this dataset (Figure 3A). Moreover, GSK1070916 ranked 9th ranked among 265 compounds ranked by confidence (P-value) in the correlation between EWS/FLI expression and sensitivity to treatment (Figure 3B). Accordingly, the average IC_{50} of Ewing sarcoma cell lines treated with GSK1070916 was significantly lower than the average IC_{50} of all other cancer cell lines screened (Figure 3C).

Next, we utilized publicly available data generated by the Broad Institute's Project Achilles to determine the relative dependency of Ewing sarcoma cell lines on Aurora kinase B expression (18). We found that Aurora kinase B ranked in the top 10% of genes sorted by the significance of hairpin depletion across Ewing sarcoma cell lines (Figure 3D). We were unable to assess the effect of Aurora kinase A in this dataset as variability in the activity of the hairpins precluded analysis. Hairpins targeting Aurora kinase C were not significantly depleted which was expected as Ewing sarcoma cell lines do not express Aurora kinase C. We also utilized a previously developed focused shRNA library targeting 449 genes, including *AURKB*, to perform an *in vivo* dependency screen in Ewing sarcoma xenografts. A673 and TC32 cells transduced with this library were injected subcutaneously in NSG mice. The tumors that developed were examined for the changes in shRNA abundance to determine which genes are necessary for tumor establishment and progression in these

models. Genes were ranked based on the significance (by P-value) of fold-change depletion of shRNA constructs targeting that gene. *AURKB* ranked 7th (out of 449 targeted genes) in the A673 *in vivo* model and scored in the top 10% (44 out of 449) of genes in the TC32 *in vivo* model (Figure 3E–F).

To further confirm the dependency of Ewing sarcoma on Aurora kinase B, we next utilized a CRISPR-Cas9 gene editing technique to target *AURKB* expression. Aurora kinase B expression was downregulated with two Aurora kinase B-specific Cas9 targeting guides (Figure 4A–B). We found that knockout of Aurora kinase B decreased phosphorylation of histone H3, a ligand of Aurora kinas B (Supplemental Figure S5A), and significantly impaired cell viability in the A673 and TC32 cell lines compared to cells treated with a non-targeting control guide ($P < 0.0001$ for all comparisons; Figure 4C). We also examined the effect of Aurora kinase B knockout on cell cycling and apoptosis. Previous studies have reported that Aurora kinase inhibition primarily induces apoptosis in *TP53*-wild-type cancer cell lines while inducing cell cycle arrest and a more delayed induction of apoptosis in *TP53*-mutated cancer cell lines (32,33). Indeed, we found that Aurora kinase downregulation in the *TP53*-mutated cell line, A673, induced cell cycle arrest in nearly 100% of the cells with evidence of endoreduplication, while 25% or less of cells exhibited induction of apoptosis. Apoptosis was induced in 40% of the *TP53*-wild-type Ewing sarcoma cells, TC32, with more modest changes in cell cycle arrest and an absence of endoreduplication (Figure 4D–E and Supplemental Figure S5B–E).

The *EWS/ETS* translocations are the only known oncogenic driver in Ewing sarcoma. To determine whether these translocations contribute to the sensitivity of Ewing sarcoma cells to Aurora kinase B inhibitors, we downregulate EWS/FLI expression with inducible shRNA. We found that cells with depleted EWS/FLI expression were resistant to concentrations of AZD-1152 that cause loss of viability in Ewing cells expressing EWS/FLI (Figure 4F). In short term cultures, we saw that downregulation of EWS/FLI expression had a mild effect on cell growth in the absence of AZD-1152 treatment, as expected (Figure 4G). One possible explanation for our results is that loss of EWS/FLI expression reduces cell growth which reduces the rate of cell cycling causing cells to be resistant to Aurora kinase B inhibition. However, Ewing sarcoma cell lines remained sensitive to AZD-1152 when cell growth was reduced by restricting fetal bovine serum (FBS) levels in the culture medium (Figure 4H–I). The only exception was in TC32 cells grown in 0% FBS, but in this case, cells had completely arrested. These studies demonstrate that the rate of cell growth cannot be the primary reason that the expression of EWS/FLI in Ewing sarcoma sensitizes cells to inhibition of Aurora kinase B.

FAK inhibition enhances the phenotypic effects of Aurora kinase B inhibition

These findings strongly support a therapeutic opportunity for targeting Aurora kinase B in Ewing sarcoma. We next examined whether the combination of FAK inhibition enhances the effects of Aurora kinase B inhibition on cell cycle arrest and apoptosis. We treated the A673 and TC32 cell lines with either control, PF-562271 alone, AZD-1152 alone, or both drugs together at concentrations corresponding to the IC_{50} (PF-562271 = 2.5 μM and AZD-1152 = 20 nM), half the IC_{50}, and one quarter of the IC_{50}. We also found that the combination of

these compounds induced a significant increase in G2 arrest using a concentration of PF-562271 (1.25 μM or half the IC_{50}) where FAK inhibition alone had no effect on cell cycle (Figure 5A–B). Similarly, apoptosis was significantly increased in both cell lines across multiple drug concentrations when comparing the combination with each compound alone (Figure 5C–D).

Combination effect of FAK with Aurora kinase B suppression confirmed with genetic approaches

We next focused on validating the synergistic activity of combining Aurora kinase B inhibition with FAK inhibition. To confirm that loss of Aurora kinase B activity sensitizes cells to FAK inhibition, we examined the effect of genetic downregulation of Aurora kinase B on sensitivity of A673 and TC32 cells to treatment with PF-562271. For these experiments, we chose an inducible shRNA system because CRISPR-Cas9 knockout of Aurora kinase B led to such a profound loss of viability that there were insufficient numbers of cells to treat with PF-562271. Downregulation of Aurora kinase B with shRNA, by contrast, significantly impaired cell viability but less profoundly than with CRISPR knockout. We found that downregulation of Aurora kinase B in A673 and TC32 cells resulted in sensitivity to lower concentrations of PF-562271 compared to cells treated with non-targeting control shRNA (Figure 5E–F). To demonstrate that FAK downregulation sensitizes Ewing sarcoma cells to Aurora kinase B inhibition, we next generated CRISPR Cas9 FAK-targeting guides that were specific for the kinase region of the gene and had no effect on expression AURKB or PYK2, a FAK homologue that is poorly expressed in A673 and TC32 (Figure 5G and Supplemental Figure S6). We found that loss of FAK expression sensitized A673 and TC32 cells to lower concentrations of AZD-1152 (Figure 5H).

Combination of FAK and Aurora kinase B inhibition downregulates mTOR activity in Ewing sarcoma

To identify a mechanisms contributing to the synergistic activity of FAK and Aurora kinase B inhibition in Ewing sarcoma cells, we analyzed the effect of these inhibitors on the phosphoproteome using a reverse phase protein array (RPPA). Ewing sarcoma cells were treated for 36 hours with two FAK inhibitors (PF-562271 and VS-4718) and two Aurora kinase B inhibitors (AZD-1152 and GSK-1070916) at the IC_{50} for each drug. Cells were treated with each drug alone and with each combination of FAK plus Aurora kinase B inhibitors and protein from cell lysates were analyzed (Supplemental Table S7). As we previously demonstrated, treatment of Ewing sarcoma cells treated with FAK inhibitors have a decrease in phosphorylated levels of S6 compared to vehicle treated control cells (7). Interestingly, we found that phosphorylation levels of S6 and several other members of the mTOR pathway, were downregulated more when cells were treated with FAK and Aurora kinase B inhibitors together than cells treated with FAK inhibitors alone (Figure 6A).

To confirm the finding that FAK and Aurora kinase inhibitors suppress mTOR pathway activity more than FAK inhibitors alone, we then treated Ewing sarcoma cells for 24 hours with VS-4718 and AZD-1152, alone and in combination, at one quarter the IC_{50} (Figure 6B) and one half the IC_{50} (Figure 6C). We chose low concentrations and a short treatment duration to make sure we were capturing on-target activity while cell viability was still

minimally impacted by treatment. Indeed, we found that the combination resulted in lower levels of phosphorylated S6 than treatment of cells with vehicle or either compound alone. The dependence of Ewing sarcoma cells on mTOR pathway activity has been well described (34,35). These results support a model where Aurora kinase B inhibition enhances the anti-Ewing effect of downregulating tyrosine kinase regulators of mTOR activity in Ewing sarcoma.

The combination of Aurora kinase B and FAK inhibition impair Ewing sarcoma tumor progression *in vivo*

To determine the effects of combining Aurora kinase B and FAK inhibition on Ewing sarcoma tumor progression *in vivo*, we first utilized an established zebrafish xenograft model of Ewing sarcoma (36). We determined that zebrafish tolerated the combination of 5 μM PF-562271 with 6 μM AZD-1152 and treatment with this combination significantly impaired tumor progression in an A673 zebrafish xenograft model of Ewing sarcoma compared to vehicle or single agent treatment. (Supplemental Figure S7A–D). We then tested the effects of the combination of PF-562271 or VS-4718 and AZD-1152 on tumor progression and survival in two mouse xenograft models of Ewing sarcoma. First, we assessed the potential for drug-drug interactions and resultant effect on the drugs' metabolism and exposure profiles. Pharmacokinetic experiments were performed with both single agent and combination dosing in NCr nude mice. No significant change in plasma exposure was observed for any of the drugs in either combination compared to their single agent arms (Supplemental Figure S7E–G). Next, we established the tolerability of the combination of 100 mg/kg PO bid of PF-562271 and 25 mg/kg IP daily of AZD-1152 for five days or 50 mg/kg PO bid of VS-4718 and 25 mg/kg IP daily of AZD-1152 in CD1 nude mice (Supplemental Figure S7H–I). We then treated Ncr nude mice, after establishment of palpable A673 xenograft tumors, with PF-562271 for 14 days and AZD-1152 on days 1–4 and 8–11. In this experiment, we chose a dose of PF-562271 that was substantially lower than we had previously used to maximize our ability to detect the synergistic activity of the combination (7). We found that the FAK inhibitor alone did not have a significant effect on tumor progression at this reduced dose, but treatment with both AZD-1152 alone and the combination treatment significantly impaired tumor progression by day 14 of treatment (Figure 6D). Furthermore, treatment with the combination ($P = 0.004$) significantly improved survival over treatment with vehicle. Treatment with the combination also improved survival compared to PF-562271 treatment alone ($P = 0.01$) and AZD-1152 treatment alone ($P = 0.02$) (Figure 6E). Finally, mice with established palpable Ewing sarcoma patient-derived xenografts (PDX) were treated with VS-4718 for 14 days and AZD-1152 on days 1–4 and 8–11. Again we found that the FAK inhibitor alone did not have a significant effect on tumor progression, but treatment with both AZD-1152 alone and the combination treatment significantly impaired tumor progression by day 21 ($P < 0.0001$; Figure 6F). However, only the mice treated with combination therapy had a significantly prolonged survival compared to vehicle treated mice ($P = 0.01$; Figure 6G).

Discussion

Despite a growing understanding of the oncogenic mechanisms that cause Ewing sarcoma, there remains a relative paucity of new candidate drug targets for the treatment of this disease. We recently identified FAK as a targetable dependency in Ewing sarcoma (7). In order to identify potential drug combinations for Ewing sarcoma that incorporate FAK inhibitors, we performed an unbiased screen of a larger collection of anti-cancer agents that includes traditional chemotherapeutic agents as well as targeted inhibitors. We found that multiple Aurora kinase inhibitors demonstrated synergistic anti-Ewing activity when combined with FAK inhibition.

Aurora kinases are serine/threonine kinases that regulate chromosomal alignment and segregation during cell division (37). Aurora kinases are frequently amplified and highly expressed in cancer (22). Thus, significant effort has been focused on developing Aurora kinase inhibitors for cancer therapy, and several inhibitors have been studied in early phase clinical trials in patients with leukemia and solid tumors (22). Aurora kinase inhibitors, including pan-Aurora inhibitors and those that selectively target Aurora kinase A or B, have been used in patients, with bone marrow suppression being the most common dose-limiting toxicity (25,26,30). Studies have also demonstrated responses and disease stabilization in patients with cancer treated with single-agent Aurora kinase inhibitors (28,30,31). Aurora kinase inhibitors are also tolerated in children, and two recent studies demonstrated efficacy for some children with aggressive solid tumors treated with an Aurora kinase A inhibitor, MLN-8237 (27,31). However, chronic exposure to these agents have induced some undesirable toxicities. In order to further improve the therapeutic window, one group has developed a nanoparticle formulation of an Aurora kinase B inhibitor (38). *In vivo* models demonstrated that this delivery approach reduces bone marrow toxicity while increasing drug exposure to the tumors. This formulation is now being tested for safety and efficacy in a clinical trial for patients with advanced solid tumors (https://clinicaltrials.gov/ct2/show/NCT02579226).

Previous studies have described a potential role for Aurora kinase inhibition in the treatment of Ewing sarcoma. Ewing sarcoma cell lines express Aurora kinase A and B, and transcript levels for both kinases correlate with EWS/FLI expression (23,24). Ewing sarcoma cell lines treated with pan-Aurora kinase inhibitors also demonstrate impaired cell viability and tumor proliferation (24). Interestingly, one study found that EWS/FLI interferes with the interaction of Aurora kinase B and wild-type EWS, impairing normal localization of Aurora kinase B during mitosis (39). Based on this finding, one might expect that Ewing sarcoma cells would be highly sensitive to further perturbations of Aurora kinase B activity. We utilized orthogonal small-molecule and functional genomic screening data combined with Aurora kinase B knockout experiments to highlight the dependency of Ewing sarcoma cells specifically on Aurora kinase B. Downregulation of EWS/FLI expression diminished the dependency of cells on Aurora kinase B activity, independent of cell growth rate, suggesting that the EWS/FLI oncogene may be directly responsible for sensitizing Ewing sarcoma to Aurora kinase B inhibitors. Furthermore, we demonstrated that single-agent Aurora kinase B inhibition impairs tumor progression and prolongs survival in a murine xenograft model of Ewing sarcoma. Our data, combined with that from previously published work, provide

support for further studies exploring the molecular mechanisms that render Ewing sarcoma cells dependent on Aurora kinase B activity.

While targeted therapy with tyrosine kinase inhibitors remains an attractive therapeutic approach in cancer, numerous studies demonstrate that single-agent therapies are unlikely to result in durable treatment responses (40,41). Our study was designed to identify drugs that could be combined with FAK inhibitors for the treatment of patients with Ewing sarcoma. Clinical trials have demonstrated that FAK inhibitors are well tolerated, and preclinical studies in mice have demonstrated tolerability of FAK inhibitors with both chemotherapy and targeted agents (42–44). Our screen nominated Aurora kinase B inhibitors for combination with FAK inhibitors in Ewing sarcoma cell lines. Several studies have also demonstrated the feasibility of combining Aurora kinase inhibitors with other anti-cancer therapies, including a study that combined an Aurora kinase B-selective inhibitor with chemotherapy (29). We found that the combination of FAK inhibition and Aurora kinase B inhibition was well tolerated in zebrafish and mice. Furthermore, we found that this combination impairs tumor progression in multiple xenograft models of Ewing sarcoma. One limitation of our study is that Aurora kinase B inhibition alone significantly impaired tumor progression in our xenograft models, limiting the ability to fully measure the additional benefit of the combination on tumor progression. However, the combination of FAK and Aurora kinase B inhibition did demonstrate an improvement in survival more than treatment with either other drug alone, providing enthusiasm for further investigating this candidate combination for Ewing sarcoma. While short-term treatment with these inhibitors prevented xenograft disease progression until treatment was withdrawn, additional studies will be needed to determine whether additional cycles of treatment can induce tumor regressions and remissions.

Finally, we utilized an unbiased proteomic screening approach to explore potential mechanisms of synergistic activity of FAK and AURKB inhibitors in Ewing sarcoma. We found that inhibiting both targets suppressed mTOR activity more than inhibition of either FAK or AURKB alone. The mTOR pathway is an important signaling mechanism within cells that senses the availability of adequate nutrients and reagents for cell growth and cell division (45). Many cancers are dependent on the mTOR pathway, including Ewing sarcoma, where both activated FAK and IGF1R promote mTOR activity (7,34,35,46). Interestingly, several studies now demonstrate that mTOR co-localizes with the chromosomal passenger complex (CPC) and AURKB, one of the core members of the CPC, during mitosis (47,48). AURKB and mTOR appear to cross regulate each other and loss of AURKB activity sensitizes cells to direct inhibition of mTOR activity by rapamycin (48,49). Therefore, one would expect that downregulation of both AURKB and tyrosine kinases that promote mTOR activity would have a synergistic anti-Ewing sarcoma effect. Indeed, our phenotypic assays demonstrate that the loss of both AURKB and FAK activity profoundly increased cell cycle arrest, supporting the theory that both AURKB and mTOR play a central role in promoting mitosis in Ewing sarcoma. Furthermore, in another recent study, IGF1R and CDK4/6 inhibitors were found to have synergistic activity in Ewing sarcoma cells acting through downregulation of the mTOR pathway (50). This combination also profoundly induced cell cycle arrest in Ewing sarcoma cells. Together, these findings suggest the possibility of a more general therapeutic opportunity in Ewing sarcoma for targeting tyrosine

kinase regulators of mTOR in combination with inhibitors of cell cycle, a hypothesis currently undergoing further investigation. With numerous inhibitors of mTOR activity in clinical investigation, including FAK and IGF1R inhibitors, and Aurora kinase B, pan-Aurora kinase, and other cell cycle inhibitors in various stages of clinical development, these classes of compounds are exciting therapeutic agents warranting further investigation for patients with Ewing sarcoma.

Supplementary Material

Refer to Web version on PubMed Central for supplementary material.

Acknowldegements:

This work was supported by the NCI 1 K08 CA188073–01A1, Team Clarkie St. Baldrick's Scholar Award, Rally Foundation, The Truth 365, Pediatric Cancer Research Foundation, Nathaniel Cavallo Fund, Team Fernando's Fight (B. Crompton); R01 CA204915, Brian MacIsaac Sarcoma Foundation and Cookies for Kids Cancer (K. Stegmaier); and the Intramural Research Program of the National Center for Advancing Translational Sciences, National Institutes of Health (NIH).

The authors thank Stephanie Meyer and Brigit McDannell for their technical assistance and the NCATS matrix team, including Sam Michael, Carleen Klumpp-Thomas, Paul Shinn, Tim Mierzwa, Lesley Griner, and Xiaohu Zhang, for their technical contributions.

References

1. Womer R, West D, Krailo M, Dickman P, Pawel B, Grier H, et al. Randomized controlled trial of interval-compressed chemotherapy for the treatment of localized Ewing sarcoma: a report from the Children's Oncology Group. J Clin Oncol 2012;30(33):4148–54 doi 10.1200/JCO.2011.41.5703. [PubMed: 23091096]
2. Grier HE, Krailo MD, Tarbell NJ, Link MP, Fryer CJ, Pritchard DJ, et al. Addition of ifosfamide and etoposide to standard chemotherapy for Ewing's sarcoma and primitive neuroectodermal tumor of bone. N Engl J Med 2003;348(8):694–701 doi 10.1056/NEJMoa020890348/8/694 [pii]. [PubMed: 12594313]
3. Delattre O, Zucman J, Plougastel B, Desmaze C, Melot T, Peter M, et al. Gene fusion with an ETS DNA-binding domain caused by chromosome translocation in human tumours. Nature 1992;359(6391):162–5 doi 10.1038/359162a0. [PubMed: 1522903]
4. Lawrence MS, Stojanov P, Polak P, Kryukov GV, Cibulskis K, Sivachenko A, et al. Mutational heterogeneity in cancer and the search for new cancer-associated genes. Nature 2013;499(7457): 214–8 doi 10.1038/nature12213. [PubMed: 23770567]
5. Crompton BD, Stewart C, Taylor-Weiner A, Alexe G, Kurek KC, Calicchio ML, et al. The genomic landscape of pediatric Ewing sarcoma. Cancer Discov 2014;4(11):1326–41 doi 10.1158/2159-8290.CD-13-1037. [PubMed: 25186949]
6. Tirode F, Surdez D, Ma X, Parker M, Le Deley MC, Bahrami A, et al. Genomic landscape of Ewing sarcoma defines an aggressive subtype with co-association of STAG2 and TP53 mutations. Cancer Discov 2014;4(11):1342–53 doi 10.1158/2159-8290.CD-14-0622. [PubMed: 25223734]
7. Crompton BD, Carlton AL, Thorner AR, Christie AL, Du J, Calicchio ML, et al. High-throughput tyrosine kinase activity profiling identifies FAK as a candidate therapeutic target in Ewing sarcoma. Cancer Res 2013;73(9):2873–83 doi 10.1158/0008-5472.CAN-12-1944. [PubMed: 23536552]
8. Sulzmaier F, Jean C, Schlaepfer D. FAK in cancer: mechanistic findings and clinical applications. Nat Rev Cancer 2014;14(9):598–610 doi 10.1038/nrc3792. [PubMed: 25098269]
9. Tai Y, Chen L, Shen T. Emerging roles of focal adhesion kinase in cancer. Biomed Res Int 2015;2015:690690 doi 10.1155/2015/690690. [PubMed: 25918719]
10. Mathews Griner L, Guha R, Shinn P, Young R, Keller J, Liu D, et al. High-throughput combinatorial screening identifies drugs that cooperate with ibrutinib to kill activated B-cell-like

diffuse large B-cell lymphoma cells. Proc Natl Acad Sci U S A 2014;111(6):2349–54 doi 10.1073/pnas.1311846111. [PubMed: 24469833]

11. Roberts W, Ung E, Whalen P, Cooper B, Hulford C, Autry C, et al. Antitumor activity and pharmacology of a selective focal adhesion kinase inhibitor, PF-562,271. Cancer Res 2008;68(6):1935–44 doi 10.1158/0008-5472.CAN-07-5155. [PubMed: 18339875]
12. Görgün G, Calabrese E, Hideshima T, Ecsedy J, Perrone G, Mani M, et al. A novel Aurora-A kinase inhibitor MLN8237 induces cytotoxicity and cell-cycle arrest in multiple myeloma. Blood 2010;115(25):5202–13 doi 10.1182/blood-2009-12-259523. [PubMed: 20382844]
13. Wilkinson R, Odedra R, Heaton S, Wedge S, Keen N, Crafter C, et al. AZD1152, a selective inhibitor of Aurora B kinase, inhibits human tumor xenograft growth by inducing apoptosis. Clin Cancer Res 2007;13(12):3682–8 doi 10.1158/1078-0432.CCR-06-2979. [PubMed: 17575233]
14. Cancer GARN, Weinstein J, Collisson E, Mills G, Shaw K, Ozenberger B, et al. The Cancer Genome Atlas Pan-Cancer analysis project. Nat Genet 2013;45(10):1113–20 doi 10.1038/ng.2764. [PubMed: 24071849]
15. Barretina J, Caponigro G, Stransky N, Venkatesan K, Margolin A, Kim S, et al. The Cancer Cell Line Encyclopedia enables predictive modelling of anticancer drug sensitivity. Nature 2012;483(7391):603–7 doi 10.1038/nature11003. [PubMed: 22460905]
16. Iorio F, Knijnenburg T, Vis D, Bignell G, Menden M, Schubert M, et al. A Landscape of Pharmacogenomic Interactions in Cancer. Cell 2016 doi 10.1016/j.cell.2016.06.017.
17. Adams ND, Adams JL, Burgess JL, Chaudhari AM, Copeland RA, Donatelli CA, et al. Discovery of GSK1070916, a potent and selective inhibitor of Aurora B/C kinase. J Med Chem 2010;53(10):3973–4001 doi 10.1021/jm901870q. [PubMed: 20420387]
18. Cowley G, Weir B, Vazquez F, Tamayo P, Scott J, Rusin S, et al. Parallel genome-scale loss of function screens in 216 cancer cell lines for the identification of context-specific genetic dependencies. Sci Data. Volume 12014 p 140035.
19. Luo B, Cheung H, Subramanian A, Sharifnia T, Okamoto M, Yang X, et al. Highly parallel identification of essential genes in cancer cells. Proc Natl Acad Sci U S A 2008;105(51):20380–5 doi 10.1073/pnas.0810485105. [PubMed: 19091943]
20. Sanjana N, Shalem O, Zhang F. Improved vectors and genome-wide libraries for CRISPR screening. Nat Methods. Volume 11(8)2014 p 783–4.
21. Tibes R, Qiu Y, Lu Y, Hennessy B, Andreeff M, Mills GB, et al. Reverse phase protein array: validation of a novel proteomic technology and utility for analysis of primary leukemia specimens and hematopoietic stem cells. Mol Cancer Ther 2006;5(10):2512–21 doi 10.1158/1535-7163.MCT-06-0334. [PubMed: 17041095]
22. Bavetsias V, Linardopoulos S. Aurora Kinase Inhibitors: Current Status and Outlook. Front Oncol 2015;5:278 doi 10.3389/fonc.2015.00278. [PubMed: 26734566]
23. Wakahara K, Ohno T, Kimura M, Masuda T, Nozawa S, Dohjima T, et al. EWS-Fli1 up-regulates expression of the Aurora A and Aurora B kinases. Mol Cancer Res 2008;6(12):1937–45 doi 10.1158/1541-7786.MCR-08-0054. [PubMed: 19074838]
24. Winter GE, Rix U, Lissat A, Stukalov A, Mullner MK, Bennett KL, et al. An integrated chemical biology approach identifies specific vulnerability of Ewing's sarcoma to combined inhibition of Aurora kinases A and B. Mol Cancer Ther 2011;10(10):1846–56 doi 10.1158/1535-7163.MCT-11-0100. [PubMed: 21768330]
25. Boss DS, Witteveen PO, van der Sar J, Lolkema MP, Voest EE, Stockman PK, et al. Clinical evaluation of AZD1152, an i.v. inhibitor of Aurora B kinase, in patients with solid malignant tumors. Ann Oncol 2011;22(2):431–7 doi 10.1093/annonc/mdq344. [PubMed: 20924078]
26. Dees EC, Cohen RB, von Mehren M, Stinchcombe TE, Liu H, Venkatakrishnan K, et al. Phase I study of aurora A kinase inhibitor MLN8237 in advanced solid tumors: safety, pharmacokinetics, pharmacodynamics, and bioavailability of two oral formulations. Clin Cancer Res 2012;18(17):4775–84 doi 10.1158/1078-0432.CCR-12-0589. [PubMed: 22767670]
27. DuBois SG, Marachelian A, Fox E, Kudgus RA, Reid JM, Groshen S, et al. Phase I Study of the Aurora A Kinase Inhibitor Alisertib in Combination With Irinotecan and Temozolomide for Patients With Relapsed or Refractory Neuroblastoma: A NANT (New Approaches to

Neuroblastoma Therapy) Trial. J Clin Oncol 2016;34(12):1368–75 doi 10.1200/jco.2015.65.4889. [PubMed: 26884555]

28. Friedberg JW, Mahadevan D, Cebula E, Persky D, Lossos I, Agarwal AB, et al. Phase II study of alisertib, a selective Aurora A kinase inhibitor, in relapsed and refractory aggressive B- and T-cell non-Hodgkin lymphomas. J Clin Oncol 2014;32(1):44–50 doi 10.1200/jco.2012.46.8793. [PubMed: 24043741]
29. Kantarjian HM, Martinelli G, Jabbour EJ, Quintas-Cardama A, Ando K, Bay JO, et al. Stage I of a phase 2 study assessing the efficacy, safety, and tolerability of barasertib (AZD1152) versus low-dose cytosine arabinoside in elderly patients with acute myeloid leukemia. Cancer 2013;119(14): 2611–9 doi 10.1002/cncr.28113. [PubMed: 23605952]
30. Lowenberg B, Muus P, Ossenkoppele G, Rousselot P, Cahn JY, Ifrah N, et al. Phase 1/2 study to assess the safety, efficacy, and pharmacokinetics of barasertib (AZD1152) in patients with advanced acute myeloid leukemia. Blood 2011;118(23):6030–6 doi 10.1182/blood-2011-07-366930. [PubMed: 21976672]
31. Mosse YP, Lipsitz E, Fox E, Teachey DT, Maris JM, Weigel B, et al. Pediatric phase I trial and pharmacokinetic study of MLN8237, an investigational oral selective small-molecule inhibitor of Aurora kinase A: a Children's Oncology Group Phase I Consortium study. Clin Cancer Res 2012;18(21):6058–64 doi 10.1158/1078-0432.ccr-11-3251. [PubMed: 22988055]
32. Ikezoe T, Yang J, Nishioka C, Yokoyama A. p53 is critical for the Aurora B kinase inhibitor-mediated apoptosis in acute myelogenous leukemia cells. Int J Hematol 2010;91(1):69–77 doi 10.1007/s12185-009-0462-7. [PubMed: 20013323]
33. Nair J, Ho A, Schwartz G. The induction of polyploidy or apoptosis by the Aurora A kinase inhibitor MK8745 is p53-dependent. Cell Cycle 2012;11(4):807–17 doi 10.4161/cc.11.4.19323. [PubMed: 22293494]
34. Mateo-Lozano S, Tirado OM, Notario V. Rapamycin induces the fusion-type independent downregulation of the EWS/FLI-1 proteins and inhibits Ewing's sarcoma cell proliferation. Oncogene 2003;22(58):9282–7 doi 10.1038/sj.onc.1207081. [PubMed: 14681687]
35. Zenali MJ, Zhang PL, Bendel AE, Brown RE. Morphoproteomic confirmation of constitutively activated mTOR, ERK, and NF-kappaB pathways in Ewing family of tumors. Ann Clin Lab Sci 2009;39(2):160–6. [PubMed: 19429803]
36. El-Naggar AM, Veinotte CJ, Cheng H, Grunewald TG, Negri GL, Somasekharan SP, et al. Translational Activation of HIF1alpha by YB-1 Promotes Sarcoma Metastasis. Cancer Cell 2015;27(5):682–97 doi 10.1016/j.ccell.2015.04.003. [PubMed: 25965573]
37. Hochegger H, Hégarat N, Pereira-Leal J. Aurora at the pole and equator: overlapping functions of Aurora kinases in the mitotic spindle. Open Biol 2013;3:120185 doi 10.1098/rsob.120185. [PubMed: 23516109]
38. Ashton S, Song Y, Nolan J, Cadogan E, Murray J, Odedra R, et al. Aurora kinase inhibitor nanoparticles target tumors with favorable therapeutic index in vivo. Sci Transl Med 2016;8(325): 325ra17 doi 10.1126/scitranslmed.aad2355.
39. Embree LJ, Azuma M, Hickstein DD. Ewing sarcoma fusion protein EWSR1/FLI1 interacts with EWSR1 leading to mitotic defects in zebrafish embryos and human cell lines. Cancer Res 2009;69(10):4363–71 doi 10.1158/0008-5472.CAN-08-3229. [PubMed: 19417137]
40. Mok T, Wu Y, Thongprasert S, Yang C, Chu D, Saijo N, et al. Gefitinib or carboplatin-paclitaxel in pulmonary adenocarcinoma. N Engl J Med 2009;361(10):947–57 doi 10.1056/NEJMoa0810699. [PubMed: 19692680]
41. Sosman J, Kim K, Schuchter L, Gonzalez R, Pavlick A, Weber J, et al. Survival in BRAF V600-mutant advanced melanoma treated with vemurafenib. N Engl J Med 2012;366(8):707–14 doi 10.1056/NEJMoa1112302. [PubMed: 22356324]
42. Hu Z, Slayton W. Integrin VLA-5 and FAK are Good Targets to Improve Treatment Response in the Philadelphia Chromosome Positive Acute Lymphoblastic Leukemia. Front Oncol 2014;4:112 doi 10.3389/fonc.2014.00112. [PubMed: 24860788]
43. Infante JR, Camidge DR, Mileshkin LR, Chen EX, Hicks RJ, Rischin D, et al. Safety, pharmacokinetic, and pharmacodynamic phase I dose-escalation trial of PF-00562271, an inhibitor

of focal adhesion kinase, in advanced solid tumors. J Clin Oncol 2012;30(13):1527–33 doi JCO.2011.38.9346 [pii] 10.1200/JCO.2011.38.9346. [PubMed: 22454420]

44. Lee Y, Lin S, Yu G, Cheng C, Liu B, Liu H, et al. Identification of Bone-Derived Factors Conferring De Novo Therapeutic Resistance in Metastatic Prostate Cancer. Cancer Res 2015;75(22):4949–59 doi 10.1158/0008-5472.CAN-15-1215. [PubMed: 26530902]
45. Sabatini DM. mTOR and cancer: insights into a complex relationship. Nat Rev Cancer 2006;6(9): 729–34 doi 10.1038/nrc1974. [PubMed: 16915295]
46. Martins AS, Mackintosh C, Martin DH, Campos M, Hernandez T, Ordonez JL, et al. Insulin-like growth factor I receptor pathway inhibition by ADW742, alone or in combination with imatinib, doxorubicin, or vincristine, is a novel therapeutic approach in Ewing tumor. Clin Cancer Res 2006;12(11 Pt 1):3532–40 doi 10.1158/1078-0432.CCR-05-1778. [PubMed: 16740780]
47. Vazquez-Martin A, Sauri-Nadal T, Menendez OJ, Oliveras-Ferraros C, Cufi S, Corominas-Faja B, et al. Ser2481-autophosphorylated mTOR colocalizes with chromosomal passenger proteins during mammalian cell cytokinesis. Cell Cycle 2012;11(22):4211–21 doi 10.4161/cc.22551. [PubMed: 23095638]
48. Song J, Salek-Ardakani S, So T, Croft M. The kinases aurora B and mTOR regulate the G1-S cell cycle progression of T lymphocytes. Nat Immunol 2007;8(1):64–73 doi 10.1038/ni1413. [PubMed: 17128276]
49. Ou O, Huppi K, Chakka S, Gehlhaus K, Dubois W, Patel J, et al. Loss-of-function RNAi screens in breast cancer cells identify AURKB, PLK1, PIK3R1, MAPK12, PRKD2, and PTK6 as sensitizing targets of rapamycin activity. Cancer Lett 2014;354(2):336–47 doi 10.1016/j.canlet.2014.08.043. [PubMed: 25193464]
50. Guenther LM, Dharia NV, Ross L, Saur Conway A, Robichaud AL, Catlett JL, et al. A combination CDK4/6 and IGF1R inhibitor strategy for Ewing sarcoma. Clin Cancer Res 2018 doi 10.1158/1078-0432.CCR-18-0372.

Translational Relevance:

Ewing sarcoma, an aggressive solid tumor affecting children, adolescents and young adults, is treated with chemotherapy, surgery, and radiation. Despite the intensity of this treatment, only a minority of patients with metastatic or recurrent disease are cured, and for long-term survivors, treatment morbidity is significant. New therapies are needed for this malignancy. In this study, we applied unbiased chemical screening to identify new candidate therapeutic combinations for this disease. Inhibitors of Aurora kinase B and focal adhesion kinase (FAK) in combination exhibited synergistic activity in multiple Ewing sarcoma models. Aurora kinase inhibitors have demonstrated tolerability and efficacy in patients with cancer, including pediatric patients with solid malignancies. With Aurora kinase B inhibitors and FAK inhibitors in clinical development, these findings have the potential to be translated to clinical trials for patients with Ewing sarcoma.

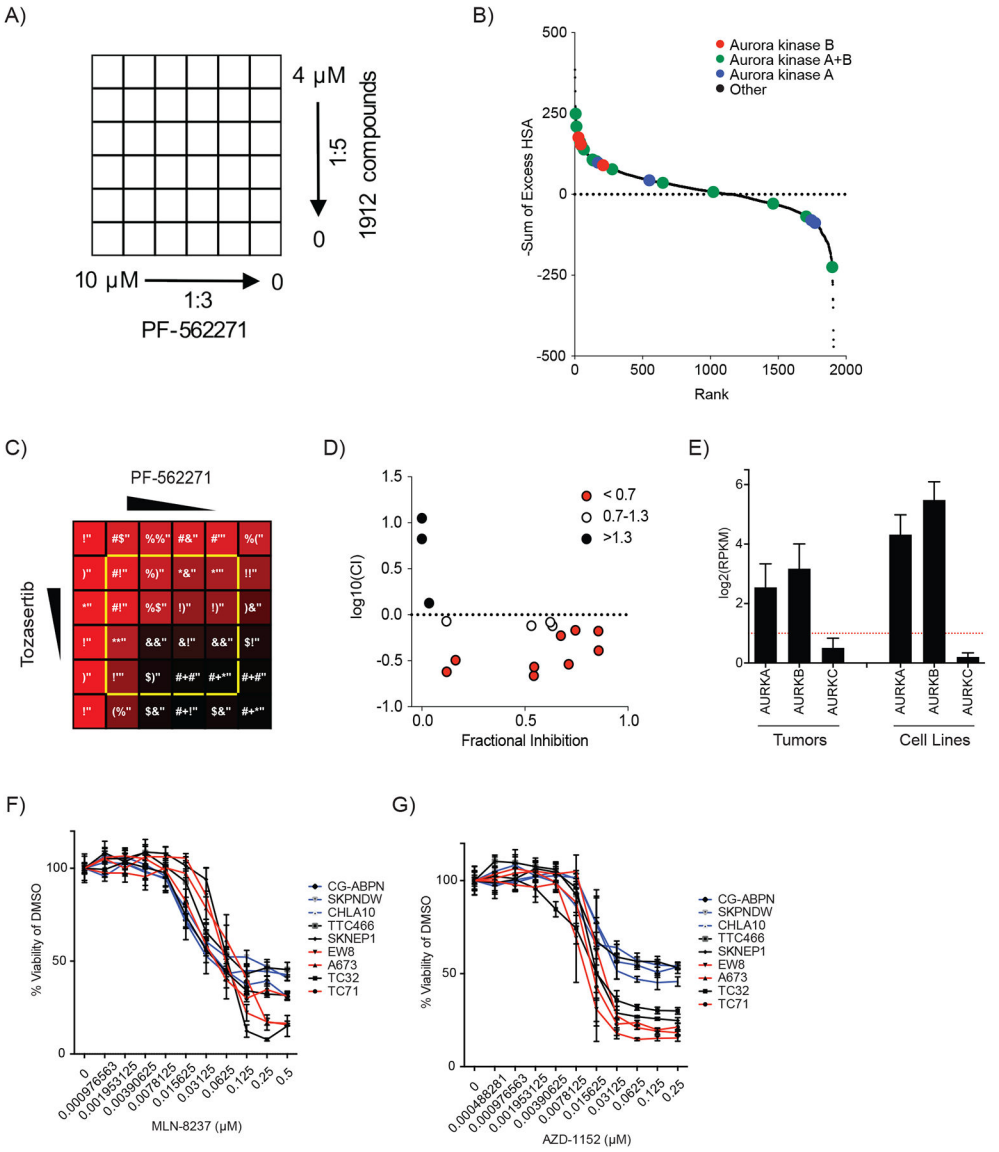

Figure 1. Screening for synergistic compounds with FAK inhibitors in Ewing sarcoma nominates the combination of FAK and Aurora kinase inhibitors

(A) Schema depicting the treatment matrix layout used in the initial screen testing the effects of compounds from the MIPE 4.0 library in combination with PF-562271 in A673 cells. **(B)** Scatter plot depicting the results of the initial synergy screen with Aurora kinase inhibitors highlighted by the indicated colors. Scores are plotted as the negative Sum of Excess over HSA for each matrix of combinations such that the highest scoring compounds rank as having the highest synergistic interactions. Scores for each combination are available in Supplemental Table S6. **(C)** Heatmap depicting screening data of the effect of combination treatment with tozasertib and PF-562271 (the top scoring Aurora kinase combination from the screen) on A673 cell viability. Color scheme depicts the effect of each combination of compound concentrations on cell viability from the greatest inhibition of viability (red) to no inhibition of viability (black) with percent viability relative to vehicle treated cells (normalized across the entire screen) in white text. Combinations plotted in panel D are

outlined in yellow. **(D)** Scatter plot of the log10 normalized Combination Index value vs. fractional inhibition of viability for each treatment combination outlined in yellow in panel C. Combinations with a CI <0.7 (indicating synergy) were plotted in red, CI = 0.7–1.3 (indicating additivity) are plotted in white, and CI >1.3 (indicating antagonism) are plotted in black. **(E)** Bar plots of Aurora kinase A, B, and C expression for 23 Ewing sarcoma tumors and 9 Ewing sarcoma cell lines. Reads per kilobase per million mapped reads (RPKM) for genes were calculated as previously reported (5). **(F-G)** Treatment dose response curves of 9 Ewing sarcoma cell lines treated for two days with **(F)** MLN-8237 or **(G)** AZD-1152. Viability was normalized to the average viability of the vehicle (DMSO) treated cells. Plotted is the mean normalized viability of four replicates +/− the SD. Cell lines are color coded by their rate of increase of relative viability when treated with vehicle (red are rapidly dividing, black are intermediate, and blue are slowly dividing) as plotted in Supplemental Figure S2A.

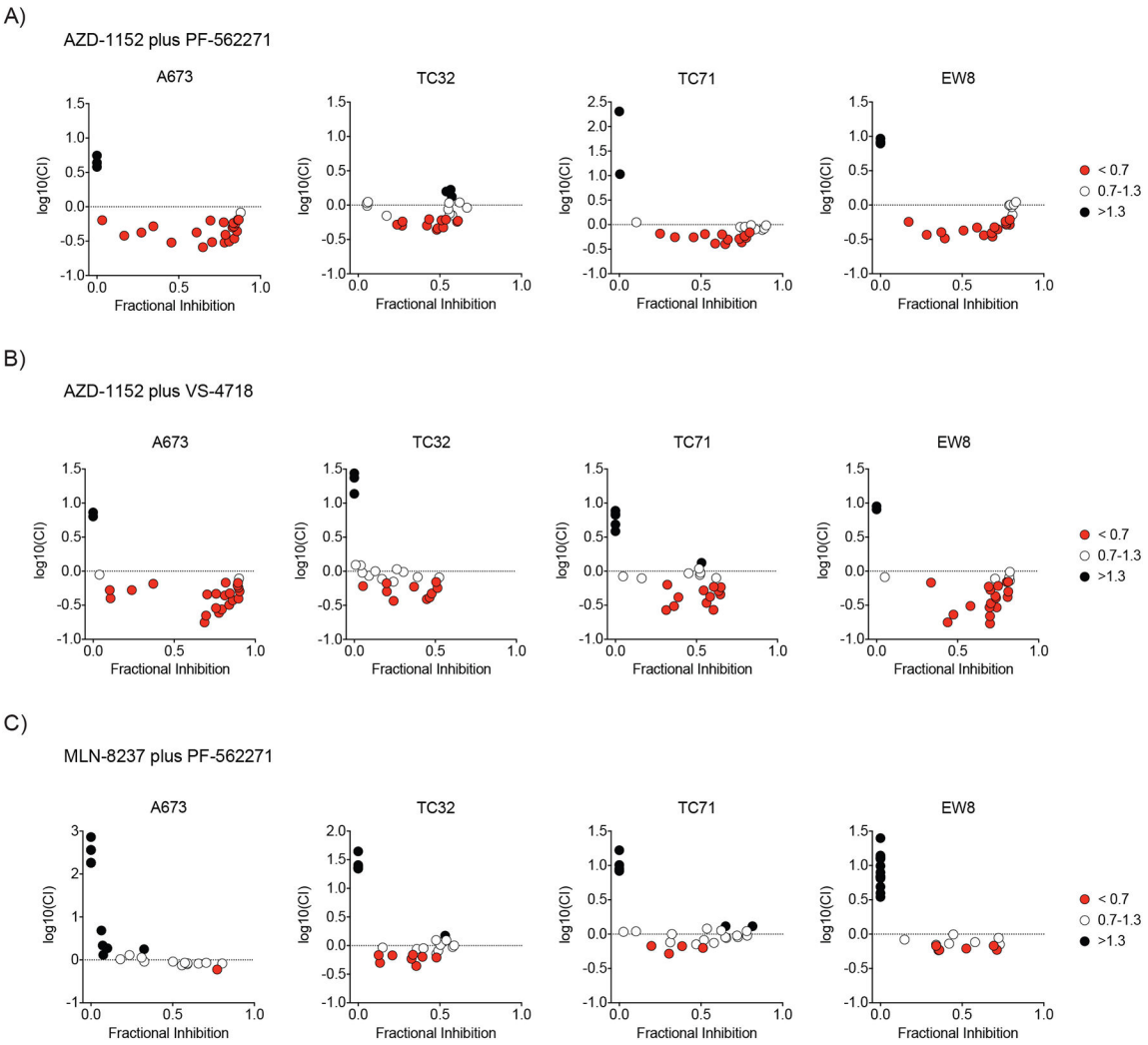

Figure 2. Aurora kinase and FAK inhibitor combinations are synergistic in Ewing sarcoma cell lines

Scatter plot of the log10 normalized Combination Index value vs. fractional inhibition of viability for each treatment combinations of **(A)** PF-562271 (FAK inhibitor) and AZD-1152 (Aurora kinase B inhibitor), **(B)** VS-4718 (FAK inhibitor) and AZD-1152, and **(C)** PF-562271 and MLN-8237 (Aurora kinase A inhibitor) for four Ewing sarcoma cell lines with an additional five lines plotted in Supplemental Figure S3. Treatment combinations that are plotted are highlighted in Supplemental Figure S4 and include the range of concentrations that are active in Ewing sarcoma cell lines (PF-562271 and VS-4718 concentrations range from 156 nM to 2.5 μM; MLN-8237 from 8nM to 125nM, and AZD-1152 from 2nM to 63nM). Combinations with a CI <0.7 (indicating synergy) were plotted in red, CI = 0.7–1.3 (indicating additivity) are plotted in white, and CI >1.3 (indicating antagonism) are plotted in black.

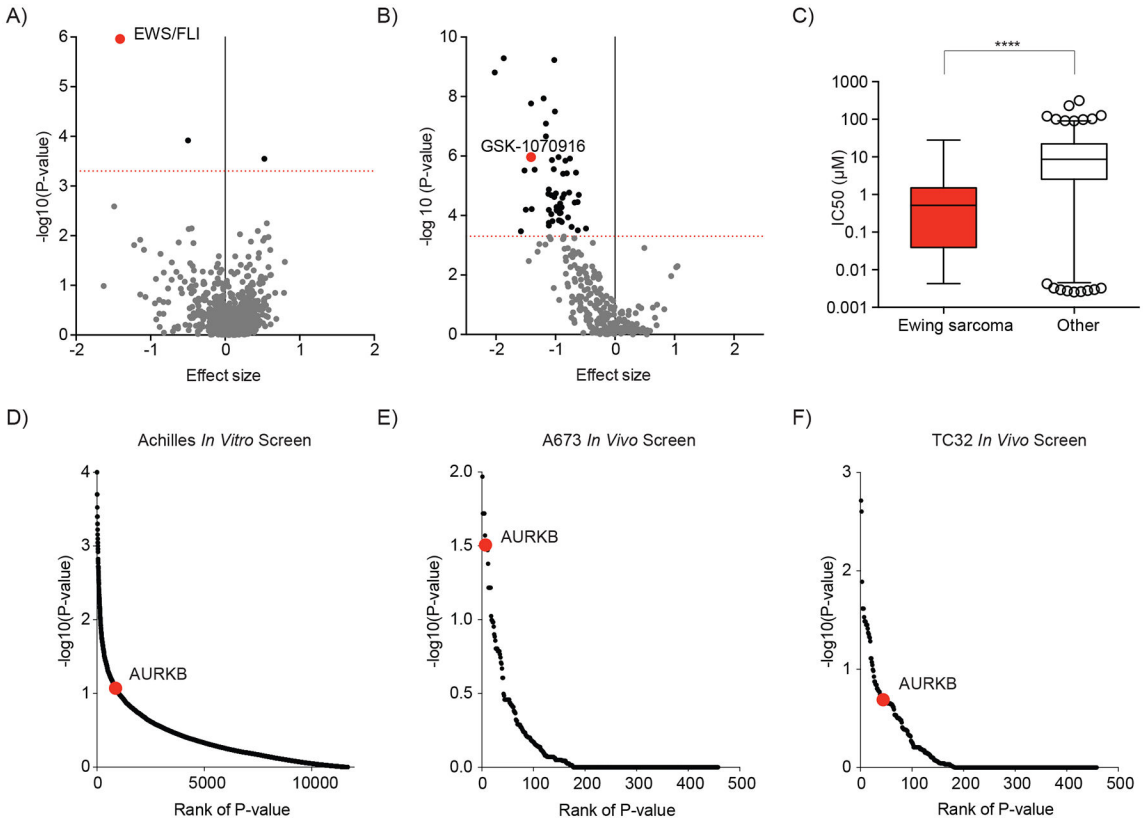

Figure 3. Ewing sarcoma cell lines are dependent on Aurora kinase B

(A-C) Data and analysis for associations between cancer features and drug sensitivity in cancer cell lines was obtained from The Genomics of Drug Sensitivity in Cancer Project (16). **(A)** Scatter plot of 690 cancer features that are associated with sensitivity or resistance to treatment with GSK-1070916 (an Aurora kinase B-selective inhibitor). The EWS/FLI cancer feature is highlighted in red. **(B)** Scatter plot of the correlation between the expression of an EWS/FLI translocation and the sensitivity of cell lines to treatment with 265 compounds. Negative effect size values indicate correlations with treatment sensitivity and positive values indicate correlations with resistance to treatment. Dotted red line indicates a P value = 0.0005. Compounds with a P value < 0.0005 are indicated by black dots, P > 0.0005 are grey. GSK-1070916, an Aurora kinase B-selective inhibitor is highlighted in red. **(C)** Box plot of IC_{50} values for 933 cell lines treated with GSK-1070916. In each box, the central line indicates the median and the box extends to the 25th and 75th percentiles. Error bars indicate the range of 1st to 99th percentiles with individual circles indicating outliers. Ewing sarcoma cell lines are compared to all other cell lines by a two-tailed Mann-Whitney test (**** P < 0.0001). **(D)** Scatter plot of the significance of Ewing sarcoma cell line dependency on expression of targeted genes in an *in vitro* genome-scale shRNA screen (18). AURKB is highlighted in red. **(E-F)** Scatter plot of the significance of **(E)** the A673 and **(F)** the TC32 Ewing sarcoma cell line dependency on expression of targeted genes for tumor progression in a mouse xenograft shRNA dependency screen targeting 449 genes. AURKB is highlighted in red.

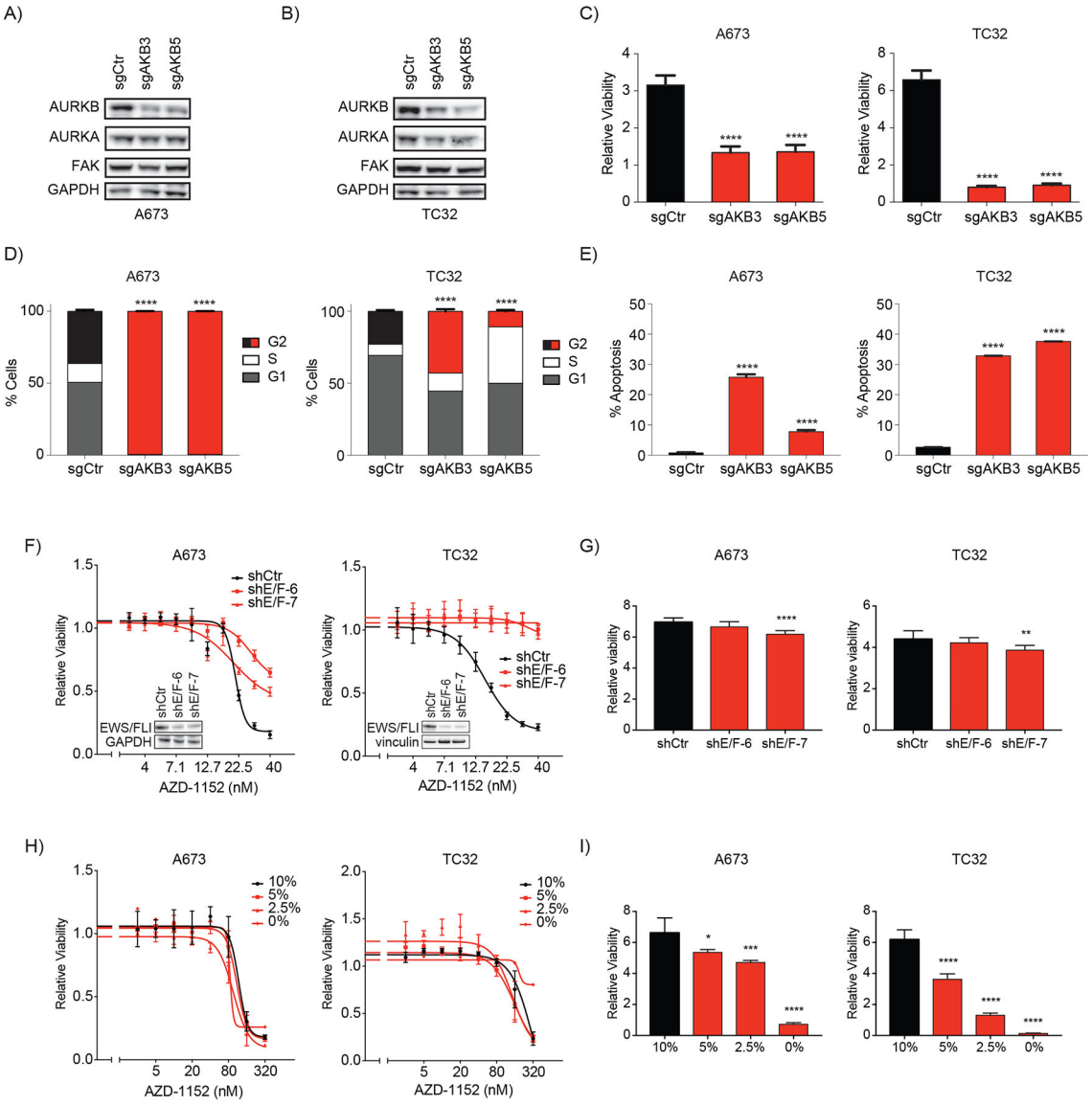

Figure 4. Phenotypic effects of Aurora kinase B knock out in Ewing sarcoma cell lines

(A-B) Western immunoblots demonstrating downregulation of AURKB expression by CRISPR-Cas9 knockout using a non-targeting control guide (sgCtr) and two AURKB targeting guides (sgAKB3 and sgAKB5) and relative stability of FAK expression. There is no effect on AURKA levels in the A673 cell lines but AURKB knockout appears to have a slight effect on AURKA levels in the TC32 cell line. **(C-D)** Effects of CRISPR-Cas9 knockout of Aurora kinase B on A673 and TC32 **(C)** cell viability, (**D)** cell cycle, and **(E)** apoptosis. For cell cycle experiments, apoptotic and dead cells were excluded from analysis. **(C)** Relative viability was calculated by dividing the day 2 viability measurement by the average day 0 viability for the same condition to demonstrate the change in viability associated with each treatment over time. Shown are the mean of eight replicates +/− SD and differences were determined by one-way ANOVA with Tukey's multiple comparisons test (**** $P < 0.0001$). **(D)** Plotted are the percentage of non-apoptotic cells +/− the 95%

confidence interval (CI) measured with DNA content equal to 2N (G1), equal to or greater than 4N (G2) or between 2N and 4N (S). G2 bars are color coded to highlight differences between control-treated cells (black) and AURKB knockout-treated cells (red). In A673, nearly all cells treated with AURKB-targeting guides are arrested in G2. Differences in the fraction of cells in G2 in each condition compared to control-treated cells were calculated by a Chi-square test (**** $P < 0.0001$). Histograms of propidium iodide staining are plotted in Supplemental Figure S5B–C**. (E)** Percentage of cells with increased Annexin V staining after knockout of Aurora kinase B. Mean percent apoptosis +/− CI are plotted as bars with AURKB knockout-treated cells colored red. Differences in each condition compared to control cells were calculated by a Chi-square test (**** $P < 0.0001$). Density plots of Annexin V staining are plotted in Supplemental Figure S5D–E**. (F)** Treatment dose response curves of A673 and TC32 Ewing sarcoma cell lines with or without downregulation of EWS/FLI expression. Cells were treated with inducible shRNA including a non-targeting hairpin (shCtr) and two EWS/FLI targeting hairpins (shE/F-6 and shE/F-7). After induction of hairpin expression, cells were treated for 3 days with AZD-1152. Western insets confirm downregulation of EWS/FLI expression at the start of treatment with AZD-1152. **(G)** Relative viability of cells treated with DMSO demonstrate a modest decrease in viability when EWS/FLI expression is downregulated. Shown are the mean of four replicates +/− SD and differences were determined by one-way ANOVA with Tukey's multiple comparisons test (**** $P < 0.0001$, ** $P < 0.01$). **(H)** Treatment dose response curves of A673 and TC32 Ewing sarcoma cell lines treated with progressively growth-restrictive amounts of FBS (normal conditions use 10%). **(I)** Relative viability of cells treated with DMSO demonstrate a significant decrease in viability when FBS is levels are decreased in the media. Shown are the mean of four replicates +/− SD and differences were determined by one-way ANOVA with Tukey's multiple comparisons test (**** $P < 0.0001$, *** $P < 0.001$, * $P < 0.05$).

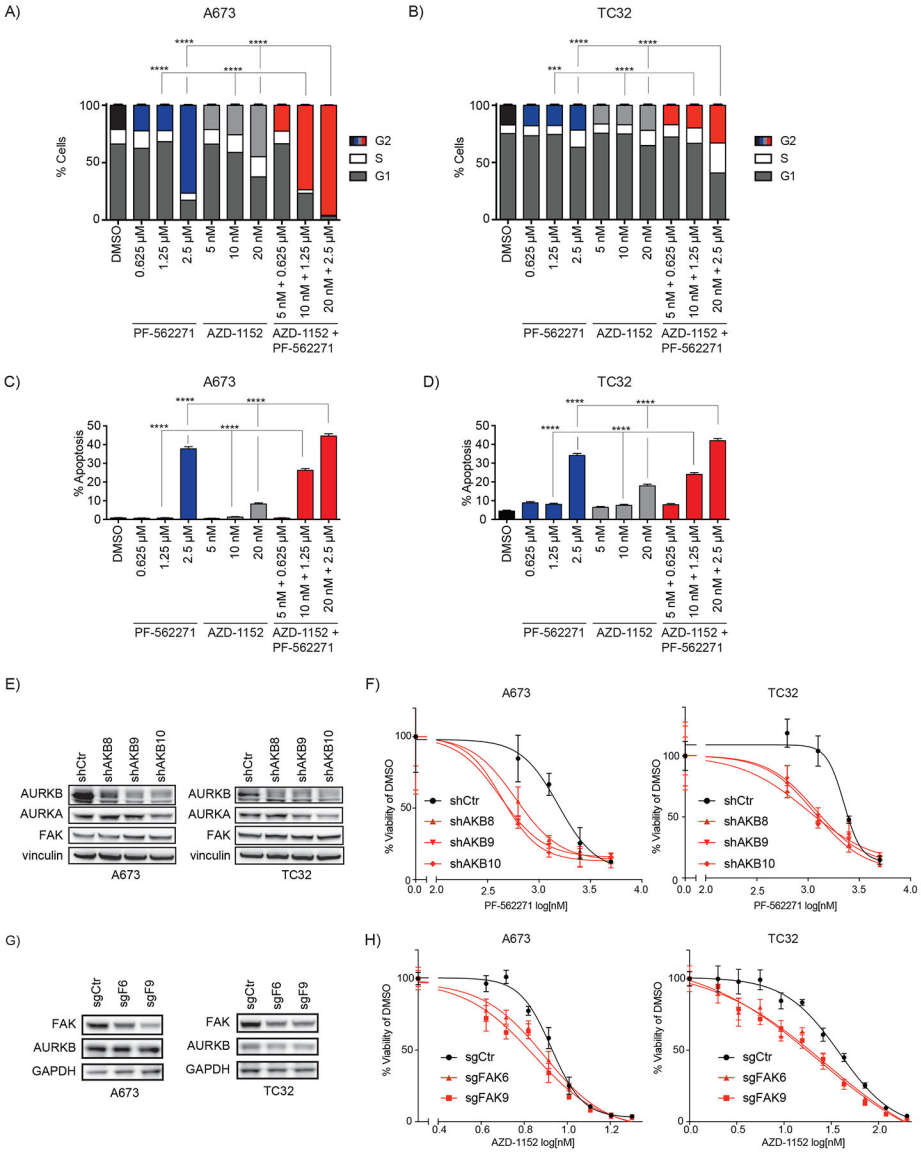

Figure 5. Phenotypic effects of combined Aurora kinase B and FAK inhibition with genetic confirmation of synergistic activity.

(A-B) Effects of treatment with PF-562271, AZD-1152, or the combination for 3 days on **(A)** A673 and **(B)** TC32 cell cycle were measured by quantifying cellular DNA content. Plotted are the percentage +/− the 95% confidence interval (CI) of non-apoptotic cells measured with a DNA content equal to 2N (G1), equal to or greater than 4N (G2) or between 2N and 4N (S). G2 bars are color coded to distinguish treatment groups such that G2 cells treated with vehicle are plotted with black bars, PF-562271-treated cells in blue, AZD-1152-treated cells in light grey, and combination-treated cells in red. Differences in the fraction of cells in G2 in each single-treatment condition were compared to cells treated with the combination at the same concentrations by a Chi-square test (*** $P < 0.001$, **** $P < 0.0001$). **(C-D)** Percentage +/− CI of measured **(C)** A673 and **(D)** TC32 cells with increased Annexin V staining after treatment with each compound alone or in combination. Bar colors indicate vehicle-treated cells (black), PF-562271-treated cells (blue), AZD-1152-treated

cells (light grey), and combination-treated cells (red). Differences in combination treatment were compared to cells treated with each compound alone at the same concentrations by a Chi-square test (**** $P < 0.0001$). **(E)** Western immunoblot demonstrates downregulation of AURKB expression in cells treated with a non-targeting shRNA hairpin (shCtr) or AURKB-targeting hairpins (shAKB8, shAKB9, shAKB10) and relative stability of AURKA and FAK expression. **(F)** Dose-response curves of A673 and TC32 cells treated with PF-562271 for three days after shRNA directed downregulation of Aurora kinase B. Plotted is the mean of four replicates +/− SD. **(G)** Western immunoblot demonstrates downregulation of FAK expression in cells treated with a non-targeting sgRNA (sgCtr) or FAK-targeting sgRNAs (sgFAK6 and sgFAK9) and relative stability of AURKB expression. **(H)** Dose-response curves of A673 and TC32 cells treated with four days of AZD-1152 after sgRNA directed knockout of FAK. Cells were. Plotted is the mean of four replicates +/− SD.

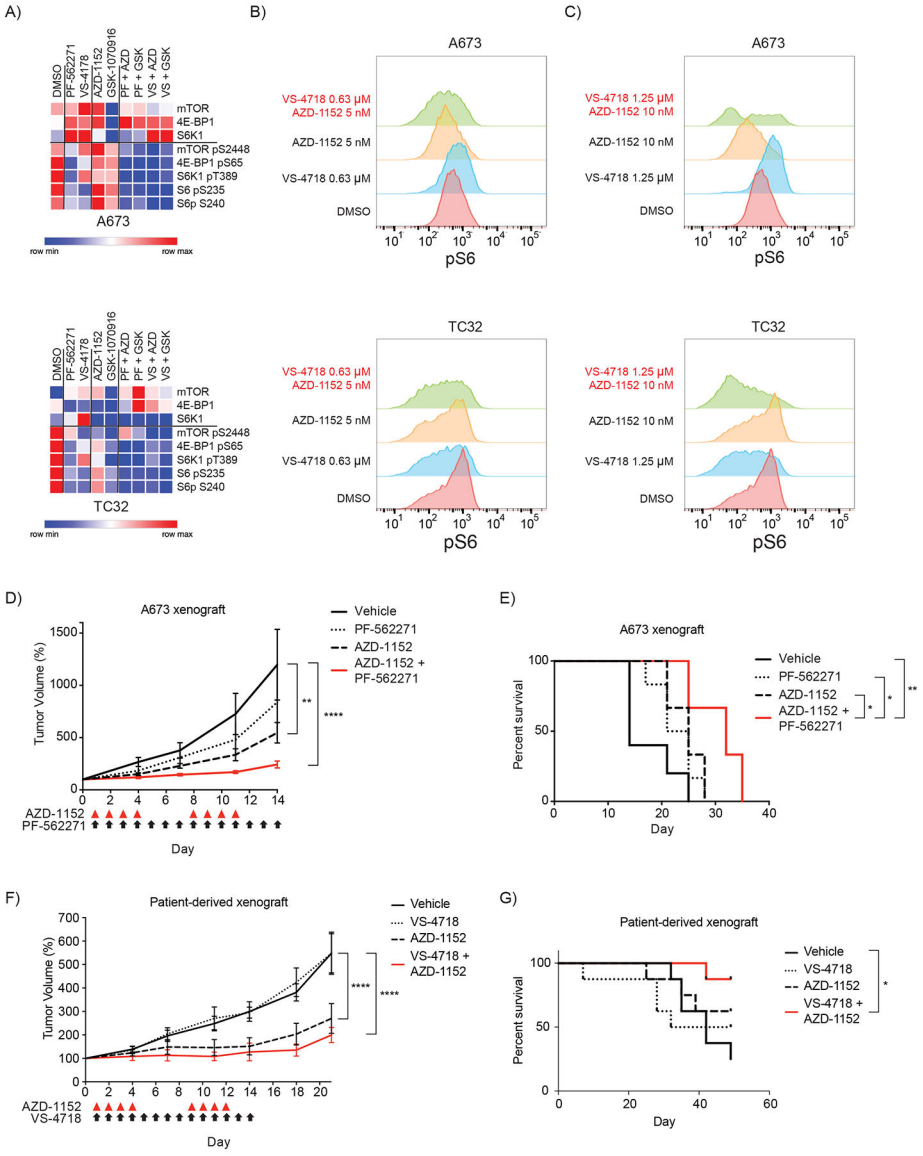

Figure 6. Phenotypic effects of combining FAK and Aurora kinase inhibition

(A) Heatmap demonstrating the effect on total protein and phosphorylation levels of members of the mTOR pathway on A673 and TC32 cells treated with vehicle, FAK inhibitors (PF-562271 and VS-4718), AURKB inhibitors (AZD-1152 and GSK-1070916) and the combination of each FAK and AURKB inhibitor as measured by RPPA. The heatmap shows scaled data where the minimum value is set to 0 and the maximum value is set to 1. The complete RPPA normalized data (unscaled) is available in Supplementary Table S7. **(B-C)** histograms of intracellular phospho-S6 (S240) levels in live cells stained with anti-phospho-S6 and measured by flow cytometry in A673 and TC32 cells treated for one day with the indicated drugs at the **(B)** one fourth of the IC_{50} concentration and **(C)** half IC_{50}. A short treatment exposure was picked for these experiments to avoid the possibility of cell death confounding the analysis of phosphorylation levels of S6. **(D)** Mean +/− SEM of subcutaneous A673 xenograft tumors in NCr nude mice treated with the indicated

compounds. Five mice were included in the control arm and six mice in each treatment arm. Day 0 indicates the day at which tumors measured at least 100 mm^3 and treatment was subsequently started on day 1. Red triangles indicate days of treatment with AZD-1152 and black arrows indicate days of treatment with PF-562271. Tumor volume measurements were continued until vehicle-treated tumors reached the institutional size limit. Volumes were compared by two-way ANOVA with Tukey's multiple comparisons test. (** $P < 0.01$, **** $P < 0.0001$). **(E)** Kaplan-Meier curves of survival of mice treated with the indicated treatment. Differences in survival were determined by log-rank test. Treatment with AZD-1152 alone ($P = 0.0398$) or the combination ($P = 0.0035$) significantly improved survival over treatment with vehicle. We also found that treatment with the combination significantly improved survival compared to PF-562271 treatment alone ($P = 0.0101$) and AZD-1152 treatment alone ($P = 0.0232$). **(F)** Mean +/− SEM of subcutaneous patient-derived xenograft (PDX) tumors in NCr nude mice treated with the indicated compounds. Eight mice were included in each arm of the study. Day 0 indicates the day at which tumors measured at least 100 mm^3 and treatment was subsequently started on day 1. Red triangles indicate days of treatment with AZD-1152 and black arrows indicate days of treatment with VS-4718. Tumor volume measurements were continued until vehicle-treated tumors reached the institutional size limit. Volumes were compared by two-way ANOVA with Tukey's multiple comparisons test. (**** $P < 0.0001$). **(G)** Kaplan-Meier curves of survival of mice treated with the indicated treatment. Differences in survival were determined by log-rank test. Treatment with the combination significantly improved survival compared to vehicle ($P = 0.0114$).